

Guidelines for the Characterization of the Internal Impedance of Lithium-Ion Batteries in PHM Algorithms

Aramis Pérez¹, Matías Benavides², Heraldo Rozas³, Sebastián Seria⁴ and Marcos Orchard⁵

^{1,2,3,4,5}*Department of Electrical Engineering, Faculty of Physical and Mathematical Sciences, University of Chile, Santiago, Chile*

*aramis.perez@ing.uchile.cl
matias.benavides@ing.uchile.cl
heraldo.rozas@ing.uchile.cl
sebastian.seria@ug.uchile.cl
morchard@ing.uchile.cl*

ABSTRACT

This article aims to describe the most important aspects to consider when using the concept of internal impedance in algorithms that focus on characterizing the degradation of lithium-ion (Li-ion) batteries. The first part of the article provides a literature review that will help the reader understand the concept of electrochemical impedance spectroscopy (EIS) and how Li-ion batteries can be represented through electrochemical or empirical models, in order to interpret the outcome of typical discharge and/or degradation tests on Li-ion batteries. The second part of the manuscript shows the obtained results of an accelerated degradation experiment performed under controlled conditions on a Li-ion cell. Results show that changes observed on the EIS test can be linked to battery degradation. This knowledge may be of great value when implementing algorithms aimed to predict the End-of-Life (EoL) of the battery in terms of temperature, voltage, and discharge current measurements. The purpose of this article is to introduce the reader to several types of Li-ion battery models, and show how the internal impedance of a Li-ion battery is a dynamic parameter that depends on different factors; and then, illustrate how the EIS can be used to obtain an equivalent circuit model and how the different electronic components vary with the use given to the battery.

1. INTRODUCTION

Since their invention, batteries have been used in a wide variety of applications that require an autonomous energy source, or just as a backup for normal operation. Regardless of how a battery is used, a typical user is interested mainly on

two things: the End-of-Discharge (EoD) time and the Remaining-Useful-Life (RUL) of the battery. These two indicators are associated to other two concepts: the State-of-Charge (SOC) and the State-of-Health (SOH). The SOC can be understood as the amount of energy that a battery can deliver until it reaches the EoD time. The SOC can be interpreted as an indicator that is particularly useful to characterize short-term operation. Meanwhile, the SOH is an indicator associated with the long-term cycle life of batteries, since every time a battery is used its RUL decreases. Both the SOC and the SOH are a function of several parameters, one of them being the internal impedance.

To understand the operation of Li-ion batteries, different types of models have been proposed; being typically categorized as empirical, electrochemical, multi-physics and molecular/atomist (Daigle & Kulkarni, 2013). The most common are electrochemical and empirical models, and different approaches can be found in the available literature, thereby several examples of them are included on this article.

Independently of the type of model that is used, it is important to note that the main purpose is to describe either how the battery cell discharges or degrades during the lifecycle. All these effects are associated with changes in the internal impedance of the battery. This impedance appears explicitly in empirical circuit models and it can be identified at different moments of the life cycle, making possible to quantify the changes of the different model parameters. In this regard, it is possible to characterize the circuit model as a transfer function of state-space structures, depending on the final application purpose (i.e., estimation or prognostics).

Thus, understanding how the internal impedance varies in time is fundamental to estimate and prognosticate the EoD and the EoL, and therefore these changes have to be considered on the modeling process. A standard practice is to consider a battery degraded when it can only deliver 75% of

Aramis Pérez et al. This is an open-access article distributed under the terms of the Creative Commons Attribution 3.0 United States License, which permits unrestricted use, distribution, and reproduction in any medium, provided the original author and source are credited.

its nominal capacity due to the changes on its internal impedance (Olivares, Cerda, Orchard, & Silva, 2013). However, understanding how the impedance changes prior to reaching that point can be helpful to determine the correct amount of energy that can be stored and delivered. The main purpose of this article can be divided in two parts. First, introduce the reader with different types of Li-ion battery models available. Then, explain the concept of EIS and how different variables affect the value of the internal impedance. Finally, an accelerated degradation experiment with its results is presented and how the EIS can be used to analyze the evolution of the different parameters that compose an internal impedance model.

2. ELECTROCHEMICAL IMPEDANCE SPECTROSCOPY

The EIS consists of a frequency response analysis of an electrochemical system when submitted to a certain electrical conditions. One of its main advantages is the amount of information that can be extracted to characterize the aging effects (Tröltzsch, Kanoun, & Tränkler, 2006). Usually the results are illustrated using a Nyquist plot with a negative Y-axis, since most electrochemical systems show a more capacitive behavior. This method is fast, non-destructive and it is a reliable technique capable of identifying the origin of the degradation process and it highlights some aging effects that traditional tests do not recognize (Vetter, Novák, Wagner, Veit, Möller, Besenhard and Hammouche, 2005). Figure 1 shows a typical Nyquist plot obtained through this technique. As proposed by these authors, the Nyquist plot can be divided in three major areas: high frequencies are associated with an inductive effect caused by the geometry of the cell and porosity of the electrode plates; the intercept with the real axis corresponds for the total value of the ohmic resistances; and the low frequency behavior can be related to the capacitive effects. Furthermore, these authors state that at low frequency ranges, where the graph may show a spike, the semicircle end corresponds to Li^+ cation diffusion in the solid-state phase. This semicircle correspond to the relaxation of charge carriers at the solid-electrolyte interface (SEI), and the other semicircle is dependent to the electrode potential, modeled by a double-layer capacitance and the charge-transfer resistance.

The diagonal line with a positive slope that starts at low frequencies on the Nyquist plot, is represented by the Warburg impedance. This impedance is associated to the result of the chemical reaction of the solid-state diffusion of the Li^+ in the bulk electrode material (Ning, Haran, & Popov, 2003). Figure 2 shows a Nyquist plot where the Warburg impedance part can be appreciated, between the 0.36 Hz and 5 mHz. As it was previously mentioned, the Nyquist plot can be approximated through different electronic components according to the frequency ranges on which these elements have a major influence. For instance, high frequencies can be represented through an inductance, while the cross by zero on the imaginary axis represents a pure resistive element. Then,

an RC-parallel branch is used to model the semicircle present on the plot. Last but not least, the Warburg impedance affects the response at low frequencies.

The adjustment of these circuits allow the transformation of visual information obtained with the Nyquist plots, into parameters that evolve in time as the degradation process becomes more evident. This way it is possible to establish a correlation between parameter changes and the SOH of the battery.

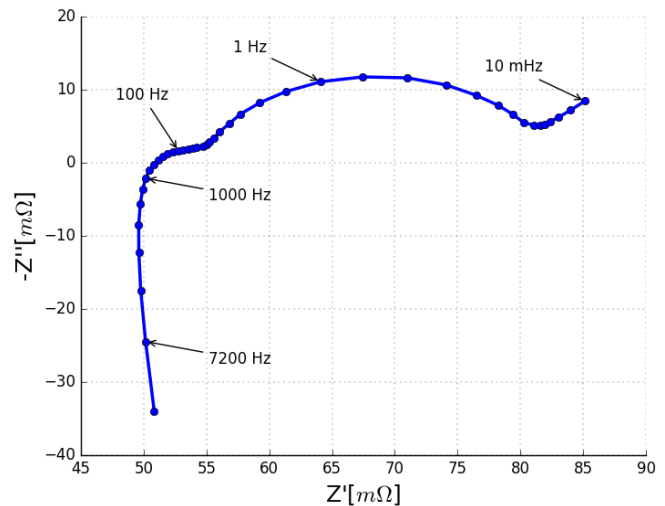


Figure 1. Typical Nyquist plot of the internal impedance of a Li-ion battery. Adapted from Vetter et al. (2005).

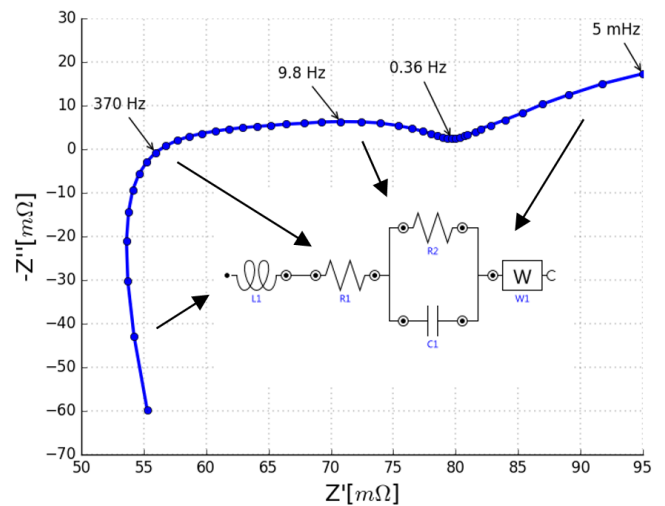


Figure 2. Nyquist plot and equivalent circuit model. Adapted from Koch and Kuhn (2014).

3. LI-ION BATTERY MODELS

3.1. Electrochemical Models

Understanding the internal chemical reactions of Li-ion batteries is essential since they have a direct influence on the

internal impedance. For this reason, modeling the electrochemical processes becomes relevant to understand the degradation process. As the name suggests, these type of models are based on electrochemical equations that represent the effects of discharge or degradation of the batteries. Usually, electrochemical models are very detailed and try to explain the stress that occurs on every component inside the battery. Ning and Popov (2004) propose a capacity fade model that includes the charge rate (CR), the depth of discharge (DOD), the end-of-charge voltage (EOCV) and the discharge rate (DR). In their paper, these authors explain through the use of partial differential equations the flow of ions from the anode to the cathode or vice-versa (depending if the battery is charging or discharging). Their results show that the degradation process that occur on the electrodes and electrolyte are the reasons of why the impedance increases throughout the lifespan.

Similarly, Daigle and Kulkarni (2013) propose a model that describes electrochemical process. These authors propose a set of equations to explain the chemical reactions that occur when the battery is being charged or discharged. Also, the authors establish different types of stress that may affect batteries when operating at low or high temperatures. For instance, at low temperatures the ionic diffusion can be compromised creating a damage such as lithium plating. In case of high temperatures, corrosion and generation of gases can occur, elevating the internal pressure. Also, the authors define four characteristics of the aging effect in the electrodes, which are: the SEI layer growth, lithium corrosion, lithium plating and contact loss. The authors emphasize how the loss of mobile ions generate an increase in the internal resistance, which is associated with a rise of the internal temperature of the battery.

Ning, White, and Popov (2006), focus on explaining a charge-discharge model, based on the loss of active Li-ions due to electrochemical reactions that occur at the anode/electrolyte interface. Hence, the rise in the anode film resistance is used to explain the decrease of the discharge voltage as battery ages. In their effort, the authors propose that the increased SEI film thickness is related to an increase of the anode film resistance.

It is understood that electrochemical models are accurate but their main disadvantage is the long simulation time that is required (Rong & Pedram, 2003). On this paper, the authors propose two electrochemical reactions that occur at each of the electrodes. Furthermore, the cycle aging is explained as an effect of cell oxidation, electrolyte decomposition, and self-discharge processes. It is important to emphasize that cell oxidation causes a film growth on the electrodes, which causes the internal resistance to rise, and this resistance is proportional to the thickness of the film. This is also supported by Santhanagopalan, Zhang, Kumaresan, and White (2008).

A study of the effects caused by how the different parts of the Li-ion battery degrade according to its use is presented by Vetter et al. (2005). In their paper, the authors propose a detailed analysis of the causes that lead to either capacity or power fade, and how it is enhanced by the different operating conditions. The work presented by these authors also support the findings made all throughout the available literature, perhaps the most important characteristic of this work is the amount of detail presented.

3.2. Empirical Models

Empirical models are built from measured data. Usually, the measured data is fitted to obtain an equivalent circuit model. Depending on the approach, the topology of this circuit can change from one study to another.

Figure 3 shows the structure proposed by Wang, He, Sun, Liu, and Wu (2011) for the equivalent model of the internal impedance of a Li-ion battery. In their work, the authors use the following elements: a resistor that represents the resistance of the electrolyte, two RC-parallel branches to represent the negative and positive pole. The RL-parallel branch is aimed to fit the data at high frequencies.

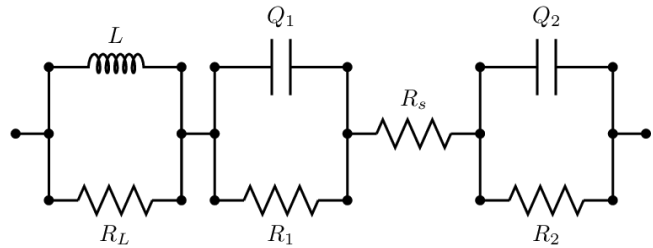


Figure 3. Equivalent circuit model of a battery. Adapted from Wang et al. (2011).

Xie, Lin, Wang, and Pedram (2012) propose a similar model; see Figure 4. In their work the authors state that the model is composed by an internal series resistance, and two parallel branches intended to model the internal capacitances.

A semi-empirical proposal is presented by Ramadass, Haran, White, and Popov (2003). In their work the authors propose a correlation to determine the state of charge and the battery resistance (polarization and film resistance) as a function of the number of cycles. Their approach includes the analysis of performance data plus a destructive physical analysis of new and cycled electrode materials. In their findings the authors establish that the capacity fade can be separated in three aspects:

- Increase of the resistance on both electrodes.
- Loss of lithiation capacity at the electrodes.
- Loss of active material in the cell.

Zou, Hu, Ma, and Li (2014) present a first-order RC model as the best choice after comparing twelve common equivalent

circuit models. This choice is based on complexity, accuracy and robustness, see Figure 5. The model consists of a series resistance and a RC branch intended to represent the diffusion effect.

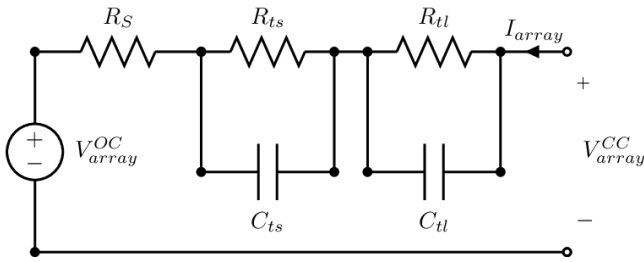


Figure 4. Li-ion battery circuit model. Adapted from Xie et al. (2012).

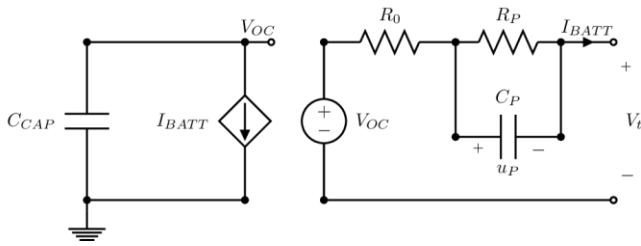


Figure 5. Battery circuit model (the left part explains the SOC, and the right part the voltage-current characteristics). Adapted from Zou et al. (2014).

3.3. Combined Electrochemical and Empirical Models

Ning, Haran, and Popov (2003) present an interesting approach where a series of analysis are performed to whole-cells and half-cells, using EIS. Also, the authors propose an experimental method to obtain the internal DC resistance of the whole-cells through the use of Ohm's Law, then their results are validated with the use of EIS on other cells. One of the major findings in their work is shown in Figure 6. This figure shows the increase of the internal resistance as a function of the depth of discharge (DOD) after 300 cycles of use. The results were obtained for cells cycled at different discharge currents, and then compared to a new cell. It is reported that the value of the resistance by the manufacturer is approximately 200 m Ω , similar to the experimental results. However near the EoD, the value of the resistance tends to increase.

A different way to analyze the changes on the battery impedance is using Nyquist plots Ning et al. (2003). In this case, instead of having a DC resistance, an AC impedance can be obtained. This AC impedance is correlated with the actual SOC, so it is very important to know the conditions under which it is measured: when fully charged the impedance of the battery is lower than when the battery is discharged. Also, as reported by the authors, a battery that is cycled at higher currents (2 or 3 times the nominal current) has higher impedance when compared to battery cycled at the

nominal current. The authors propose the use of Croce's model to analyze the EIS results shown in Figure 7. The idea behind this model is that on the Nyquist plots there are three semi-circles that can be noted, depending if the area corresponds to high, medium or low frequencies. High frequencies are associated with the migration of active material through the SEI, at middle frequencies the semi-circle is associated to the charge-transfer resistance across the interface; and, finally, low frequencies, are related to the resistance of the electrode material (Ning et al., 2003). Furthermore the slope that can be obtained at low frequencies represents a characteristic associated with the Warburg diffusion region. Additionally, the authors propose an equivalent circuit model that represents the obtained data with the EIS, on Figure 8. For this model, R_{elec} represents the resistance of the active material in the electrolyte. The RC branches are associated to the passivating surface layer, the charge-transfer and the electronic resistance of the material respectively. Also, the Warburg impedance and the capacitance are considered to have an effect only at very low frequencies.

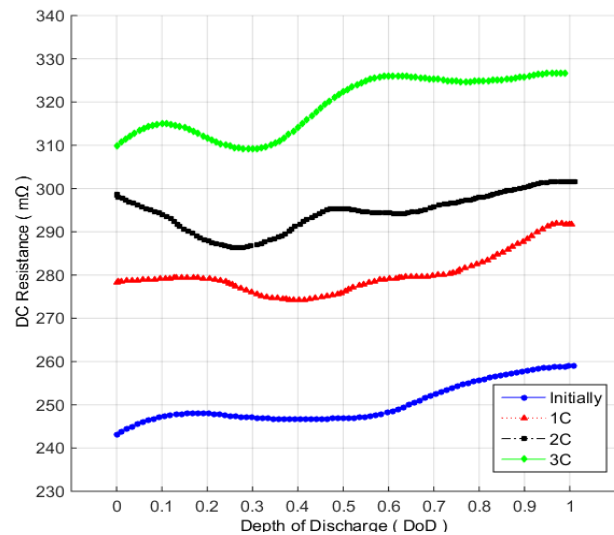


Figure 6. DC Resistance as a function of DOD. Adapted from Ning et al. (2003).

A simpler circuit equivalent model obtained through EIS is presented by Saha, Goebel, Poll, and Christophersen (2009) on Figure 9. In this case C_{DL} represent a double layer capacitance, R_{CT} is the charge transfer resistance, R_W stands for the Warburg impedance and R_E is the electrolyte resistance. In their work the authors also propose the use of a semi-circle on the Nyquist plot in order to find the parameters.

Dai, Wei, and Sun (2009) performed a similar experiment. In their proposal, Li-ion batteries were cycled under different conditions causing a variation of the ohmic resistance. Figure 10 shows how the authors define the evolution of the ohmic and the polarization resistances. The importance of this figure is to note how the polarization resistances is practically

constant while the ohmic resistance does change with cycling. Since this resistance tends to increase, the authors, propose to study it in order to understand better the SOH.

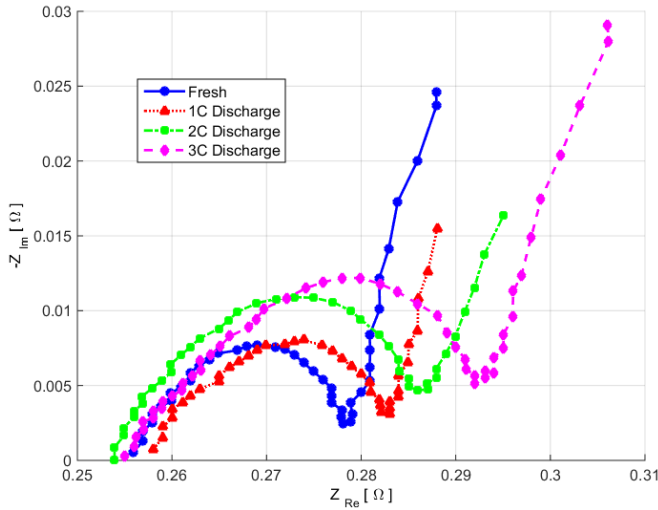


Figure 7. Nyquist plot for a new battery and for used batteries after 300 cycles and 100% SOC. Adapted from Ning et al. (2003).

Figure 11 shows another experiment that was performed. The intention was to measure the ohmic resistance variation (defined as R/R_{new}) when the battery was discharged at different multiples of the nominal current and at a temperature of 40 °C. It is easily seen that the resistance increases at higher currents.

Since not all cycles are the same, the authors also include the ohmic resistance variation when the battery is discharged at different values of DOD. In this case also, the temperature is 40 °C and the charge and discharge current is equal to the nominal value or 1C. Figure 12 shows that, the higher DOD cycles have a major impact on the resistance than a more conservative use.

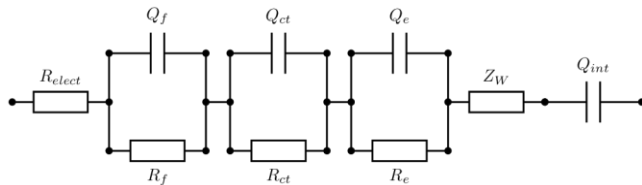


Figure 8. Equivalent circuit model obtained through EIS. Adapted from Ning et al. (2003).

The last result presented by Dai et al. (2009) is an analysis of the ohmic resistance variation, as a function of the temperature when charging and discharging at nominal current. Figure 13 illustrates that the operating temperature

has a major impact since the variation trend increases as the temperature is higher.

With these findings, the authors propose the model of Figure 14. The series resistance is used to describe the internal ohmic resistance. The RC branches are used to represent polarization effects, while C_E is a combination of a capacitance and voltage source that depends on the SOC and open circuit voltage.

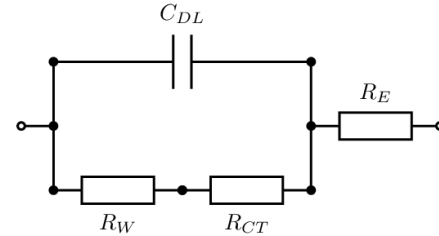


Figure 9. Battery equivalent circuit model. Adapted from Saha et al. (2009).

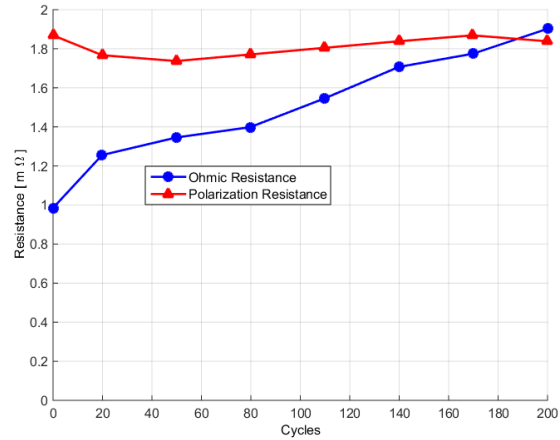


Figure 10. Ohmic and polarization resistance. Adapted from Dai et al. (2009).

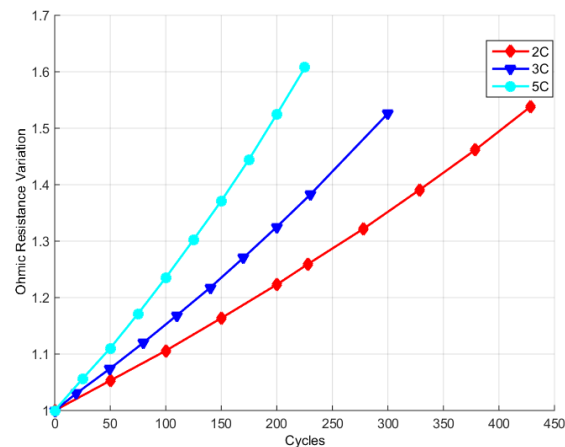


Figure 11. Ohmic resistance variation when cycled at different currents. Adapted from Dai et al. (2009).

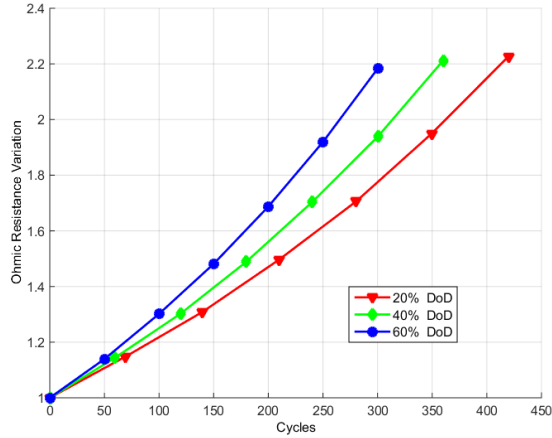


Figure 12. Ohmic resistance variation when cycled at different DODs. Adapted from Dai et al. (2009).

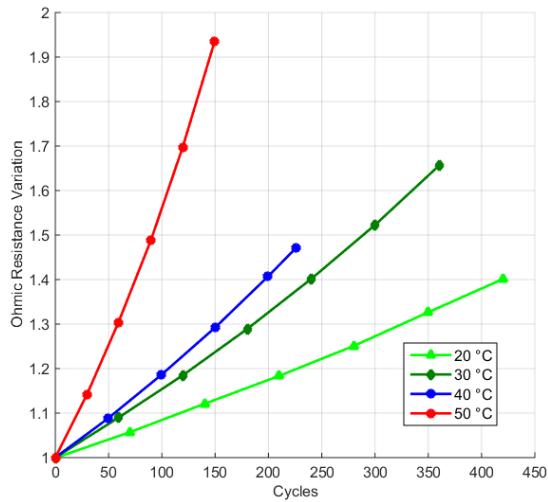


Figure 13. Ohmic resistance variation when cycled at different temperatures. Adapted from Dai et al. (2009).

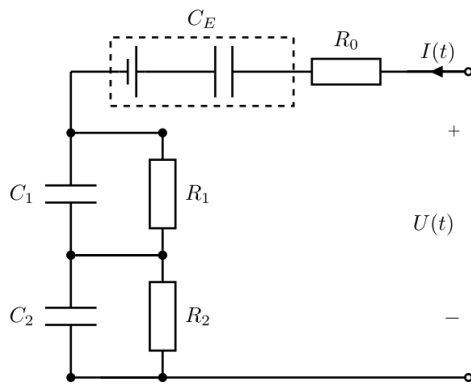


Figure 14. Equivalent circuit model. Adapted from Dai et al. (2009).

4. EXPERIMENTAL TESTS AND OBTAINED RESULTS

The following results aim to illustrate how the degradation process can be studied through the use of EIS and the corresponding Nyquist plots that are generated with this method. Measured data is used to fit two empirical models; one of them offering a more complex structure and, therefore, more parameters. Also, with the Nyquist plots it is possible to determine how the internal impedance varies through cycling, creating a map between the curve and the ohmic resistance value. This concept was experimentally validated using data from a continuous cycling test performed on Panasonic CGR18650CG Li-ion battery cells (nominal capacity 2250 mAh, and a cut-off voltage of 3 V). The charging protocol was the constant current-constant voltage (CCCV) method, and the temperature was controlled at a room temperature of 25 °C.

The first 10 cycles were executed at nominal current to allow a proper electrochemical stabilization of the battery. Afterwards, the EIS test was performed every 20 cycles, when the battery was fully charged, and at 25 °C. The galvanostatic mode was set on, the current amplitude was 50 mA, and the frequency range was between 10 kHz and 5 mHz, with 7 seven measurements per decade.

Figure 15 shows the different Nyquist plots obtained throughout the cycling procedure. The initial state curve shows the brand new cell completely charged before any discharge. The other curves show the different Nyquist plots every 100 cycles. It can be observed that the curve displaces to the right on the real axis, until it reaches a point at cycle 480, where the capacity of the battery reaches an 80% of its original value, at nominal current.

Figure 16 shows how the ohmic resistance varies through the cycling experiment. This value is obtained at 370 Hz, which corresponds to the cross by zero on the imaginary axis. At the beginning of the experiment, the value of the experiment is bounded and has small variations, but as the amount of cycles increases, the changes on the resistance also increases. Even more, it is possible to see a major increase on the resistance after 450 cycles. At this point the nominal capacity of the battery is near an 80% of its original value.

Using the experimental data, we are going to focus on three measured cases. With this measurements, we are going to fit the Nyquist plot and generate the equivalent empirical circuit model. The intention is to study the changes on the circuit parameters to determine which of them have a significant variance, when compared to the initial values of the cell prior to start the cycling experiment. In this approach we are presenting two empirical models for comparison purposes. We are focusing on three specific cycles: cycle 0 (new battery), cycle 310 (manufacturer reports information up to cycle 300) and cycle 480 (almost an additional 50% of cycles). The value of the ohmic resistance for these cycles are: $R_0 = 52.7 \text{ m}\Omega$, $R_{310} = 54.6 \text{ m}\Omega$, and $R_{480} = 56.8 \text{ m}\Omega$.

Figure 17 shows the Nyquist plot of the measured data and the fitted curve that corresponds to the equivalent circuit shown in Figure 18. In this case, it can be observed that the fitted curve is not very accurate when compared to the measured data. This means that the selection of the particular empirical simple model perhaps might not be a good choice when trying to understand the evolution of the impedance of the battery.

Table 1 shows the different values of the parameters for the three fitted curves. From the results shown on this table, it is possible to see that the changes on the value of the parameters are considerable. It is important to mention that the value of the R1 resistor is very close to the measured ohmic resistance in Figure 16.

A second fit was approached using a different circuit model. The Nyquist plot can be seen on Figure 19. In this case, the fitted curve is more accurate when compared to the real data. This means that the empirical model can represent the dynamics of the battery on a better way.

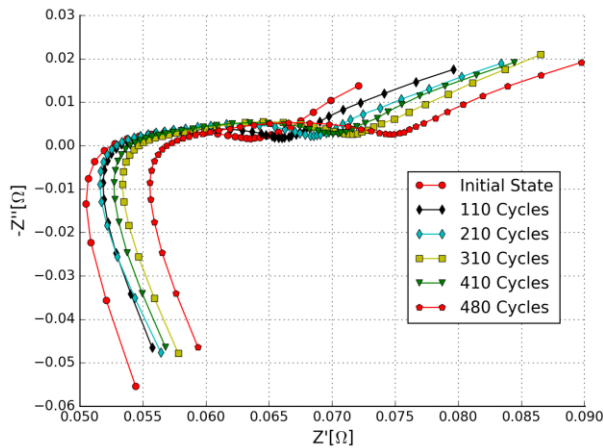


Figure 15. Nyquist plots at different cycles for the performed experiment.

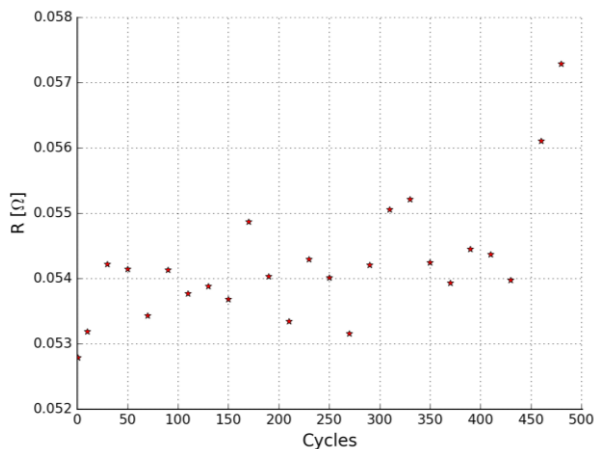


Figure 16. Resistance value at different cycles.

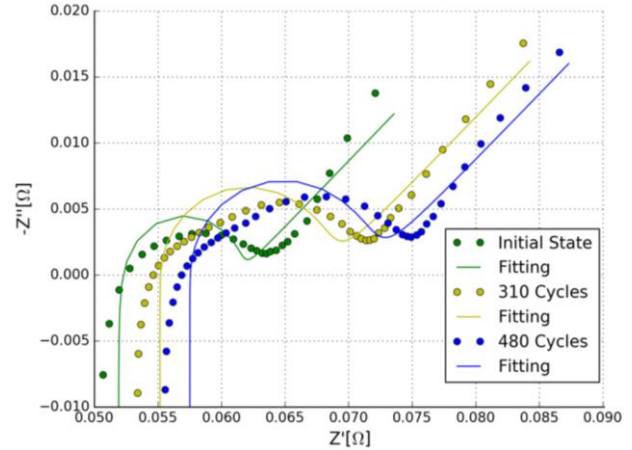


Figure 17. Nyquist plots for measured and fitted data of Model #1.

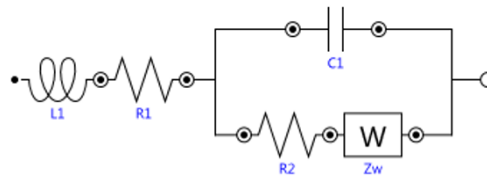


Figure 18. Equivalent empirical circuit Model #1.

Element	Cycle #0	Cycle #310	Cycle #480
L1 (nH)	883	716	694
R1 (mΩ)	51.9	55.2	57.5
R2 (mΩ)	9.48	13	13.9
C1 (F)	0.245	1.06	1.26
Zw (S)	231	209	212

Table 1. Circuit parameters for empirical Model #1

Figure 20, shows the equivalent model obtained for this case. It is important to mention that the two RC branches connected in series with the resistor R3, correspond to an equivalent topology that emulates the effect of the Warburg impedance (Do, Forgez, Benkara, & Friedrich, 2009) (Mauracher & Karden, 1997). Furthermore, Table 2 shows the different values for all the elements for each cycle of operation. Similar to the previous model, the resistor R1 has a value near the measured value of the ohmic resistance. This means, that regardless of the model, the ohmic resistance is very similar to the actual value.

In this case, Model #2 fits in a better way the measured data, although the variations on the values of the elements is very high except for R2. These models were obtained with the software Nova 2, property of Metrohm Autolab, which allows an option of “Fit and Simulation of equivalent circuit models” through the use of EIS. The two models presented in this article are included in the available options of the software. In this regard, the values of the parameters are optimized using nonlinear least squares to fit the

experimental values. Even though the empirical model has many parameters, it is important to keep in mind that each element has a definite contribution on different frequency ranges. If the Nyquist plots are compared it can be seen that Model #2, (which has more parameters) fits the real data in a better manner than Model #1. Hence, Model #2 is able to capture in a better manner the complete range of dynamics of the battery without overfitting the model. Furthermore, the chi-square test for Model #1 has a value of 0.19504, while for Model #2 the value is 0.0020974.

Figure 21 shows how nominal capacity of the studied Panasonic Li-ion battery decreases at the same time that the ohmic resistance increases. This plot is built in chronological order, this means that when the capacity degradation is equal to 1, the battery is fresh, while the last point corresponds to the parameters of capacity and resistance after 760 cycles. After the first 300 cycles of the experiment, it is noted that a variation of 3% on the value of the resistance produces a reduction of nearly 14% of the total capacity. After this point, the variation on the delivered capacity remains almost constant, but internally the battery is changing since the increment on the resistance is significant, approximately 8% of the original value. An interesting phenomena can be observed towards the end, where the capacity drops from nearly 82% until 75%, associated to a 2 mΩ increment on the resistance, growing from 56.8 mΩ and reaching 58.7 mΩ. In this case, a total reduction of 25% of the nominal capacity is associated to an increment of 11% of the original value of the resistance.

For reference purposes a third degree polynomial fit curve is also included in Figure 21. Although more experimentation and data are required to validate a specific structure to support this trend for any event, it is interesting to show this characteristic. For this reason, this analysis is left for future research.

Table 3 shows the normalized capacity and resistance value for several cycles.

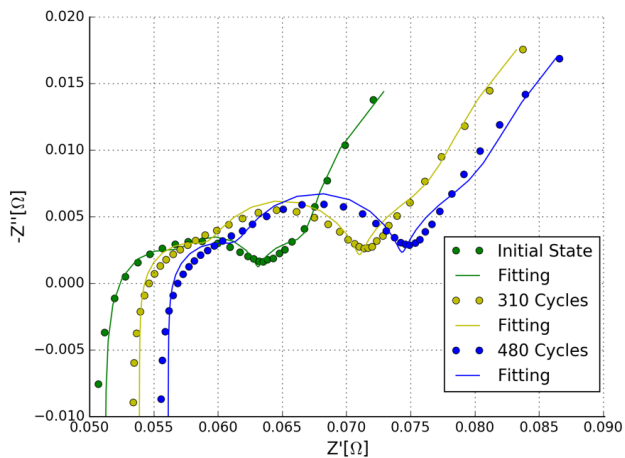


Figure 19. Nyquist plots for measured and fitted data of Model #2.

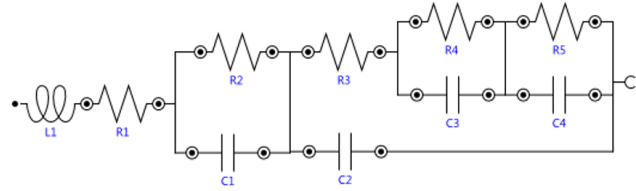


Figure 20. Equivalent empirical circuit Model #2.

Element	Cycle #0	Cycle #310	Cycle #480
L1 (nH)	890	759	738
R1 (mΩ)	51.20	53.90	56.10
R2 (mΩ)	5.71	5.43	5.38
R3 (mΩ)	6.34	11.90	13.00
R4 (mΩ)	3.78	5.92	6.35
R5 (mΩ)	39.70	50.40	49.90
C1 (mF)	124	300	319
C2 (F)	1.68	3.01	3.20
C3 (F)	222	530	579
C4 (F)	954	1200	1270

Table 2. Circuit parameters for empirical Model #2.

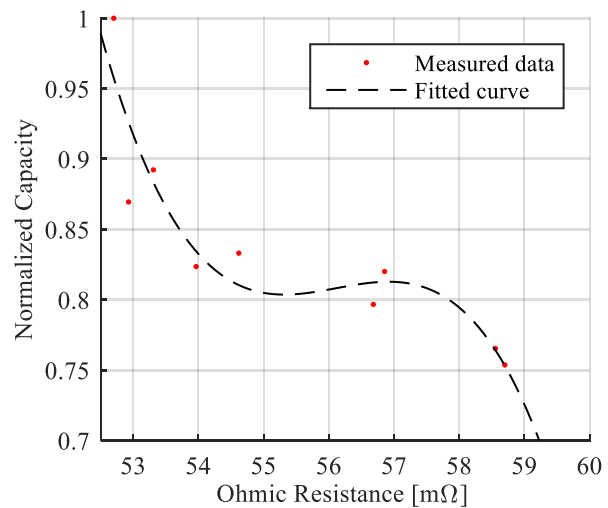


Figure 21. Normalized capacity with its corresponding value of ohmic resistance.

Cycle	Normalized Capacity	Ohmic Resistance (mΩ)
0	1	52.7
132	0.89224	53.309
202	0.86945	52.927
311	0.83307	54.618
412	0.82357	53.964
462	0.82004	56.855
550	0.79667	56.682
700	0.7653	58.555
760	0.7536	58.7

Table 3. Variations of the capacity and resistance at different cycles.

5. CONCLUSIONS

This paper presents a background on basic terminology associated with Li-ion batteries. Also, the components of this type of batteries are explained, as well as a brief introduction of the different types of resistances that can be located inside the batteries. Even though, sometime the literature refers to Li-ion batteries as a generic product, it is important to know that different chemistries are available on the market, and the purposes of the batteries can be different.

The use of EIS, a non-invasive method, is very helpful in order to understand the inside of the batteries. The main disadvantage of this method is the cost of the equipment. However, empirical circuit models can be used to represent the dynamics of the batteries. Empirical circuit models can be found on the available literature, and some models are more complex than others.

The experimental results, show that first order circuits are too basic when used to explain the equivalent impedance of a Li-ion battery. In our case, a third order model (where the two RC branches that emulate the Warburg impedance are fused into one branch) fits better the measured data. However, some models might neglect this effect since this impedance only affects low frequencies.

Finally, it is important to note that, regardless of the model that is used, the ohmic resistance is generally very close to the value that is directly measured in laboratory tests.

ACKNOWLEDGEMENTS

This work has been partially supported by FONDECYT Chile Grant Nr. 1170044, and the Advanced Center for Electrical and Electronic Engineering, AC3E, Basal Project FB0008, CONICYT. The work of Aramis Perez was supported by the University of Costa Rica (Grant for Doctoral Studies) and CONICYT-PCHA/Doctorado Nacional/2015-21150121. The work of Heraldo Rozas was supported by CONICYT-PFCHA/Magister Nacional/2018-22180232.

REFERENCES

- Dai, H., Wei, X., & Sun, Z. (2009). A new SOH prediction concept for the power lithium-ion battery used on HEVs. In *5th IEEE Vehicle Power and Propulsion Conference, VPPC '09* (pp. 1649–1653). IEEE. <https://doi.org/10.1109/VPPC.2009.5289654>
- Daigle, M., & Kulkarni, C. (2013). Electrochemistry-based Battery Modeling for Prognostics. *Annual Conference of the Prognostics and Health Management Society*, 1–13.
- Do, D. V., Forgez, C., Benkara, K. E. K., & Friedrich, G. (2009). Impedance observer for a Li-ion battery using Kalman filter. *IEEE Transactions on Vehicular Technology*, 58(8), 3930–3937.
- Koch, R., & Kuhn, R. (2014). Electrochemical Impedance Spectroscopy for Online Battery Monitoring - Power Electronics Control. In *Power Electronics and Applications (EPE'14-ECCE Europe), 2014 16th European Conference on* (pp. 1–10). IEEE.
- Mauracher, P., & Karden, E. (1997). Dynamic modelling of lead/acid batteries using impedance spectroscopy for parameter identification. *Journal of Power Sources*, 67(1–2), 69–84.
- Ning, G., Haran, B., & Popov, B. N. (2003). Capacity fade study of lithium-ion batteries cycled at high discharge rates. *Journal of Power Sources*, 117(1–2), 160–169. [https://doi.org/10.1016/S0378-7753\(03\)00029-6](https://doi.org/10.1016/S0378-7753(03)00029-6)
- Ning, G., & Popov, B. N. (2004). Cycle Life Modeling of Lithium-Ion Batteries. *Journal of The Electrochemical Society*, 151(10), A1584. <https://doi.org/10.1149/1.1787631>
- Ning, G., White, R. E., & Popov, B. N. (2006). A generalized cycle life model of rechargeable Li-ion batteries. *Electrochimica Acta*, 51(10), 2012–2022. <https://doi.org/10.1016/j.electacta.2005.06.033>
- Olivares, B. E., Cerda Muñoz, M. A., Orchard, M. E., & Silva, J. F. (2013). Particle-filtering-based prognosis framework for energy storage devices with a statistical characterization of state-of-health regeneration phenomena. *IEEE Transactions on Instrumentation and Measurement*, 62(2), 364–376. <https://doi.org/10.1109/TIM.2012.2215142>
- Ramadass, P., Haran, B., White, R., & Popov, B. N. (2003). Mathematical modeling of the capacity fade of Li-ion cells. *Journal of Power Sources*, 123(2), 230–240. [https://doi.org/10.1016/S0378-7753\(03\)00531-7](https://doi.org/10.1016/S0378-7753(03)00531-7)
- Rong, P., & Pedram, M. (2003). An analytical model for predicting the remaining battery capacity of lithium-ion batteries. *Proceedings -Design, Automation and Test in Europe, DATE*, 14(5), 1148–1149. <https://doi.org/10.1109/DATE.2003.1253775>
- Saha, B., Goebel, K., Poll, S., & Christophersen, J. (2009). Prognostics Methods for Battery Health Monitoring Using a Bayesian Framework. *IEEE Transactions on Instrumentation and Measurement*, 58(2), 291–296. <https://doi.org/10.1109/TIM.2008.2005965>
- Santhanagopalan, S., Zhang, Q., Kumaresan, K., & White, R. E. (2008). Parameter Estimation and Life Modeling of Lithium-Ion Cells. *Journal of The Electrochemical Society*, 155(4), A345. <https://doi.org/10.1149/1.2839630>
- Tröltzsch, U., Kanoun, O., & Tränkler, H.-R. (2006). Characterizing aging effects of lithium ion batteries by impedance spectroscopy. *Electrochimica Acta*, 51(8), 1664–1672.

- Vetter, J., Novák, P., Wagner, M. R., Veit, C., Möller, K. C., Besenhard, J. O., ... Hammouche, A. (2005). Ageing mechanisms in lithium-ion batteries. *Journal of Power Sources*, 147(1–2), 269–281. <https://doi.org/10.1016/j.jpowsour.2005.01.006>
- Wang, H., He, L., Sun, J., Liu, S., & Wu, F. (2011). Study on correlation with SOH and EIS model of Li-ion battery. In *Proceedings of the 6th International Forum on Strategic Technology, IFOST 2011* (Vol. 1, pp. 261–264). IEEE. <https://doi.org/10.1109/IFOST.2011.6021018>
- Xie, Q., Lin, X., Wang, Y., & Pedram, M. (2012). State of health aware charge management in hybrid electrical energy storage systems. In *Design, Automation & Test in Europe Conference & Exhibition (DATE), 2012* (pp. 1060–1065). EDA Consortium. Retrieved from <http://dl.acm.org/citation.cfm?id=2492970>
- Zou, Y., Hu, X., Ma, H., & Li, S. E. (2014). Combined SOC and SOH estimation over lithium-ion battery cell cycle lifespan for Electric vehicles. *Journal of Power Sources*, 273(January), 793–803. <https://doi.org/10.1016/j.jpowsour.2014.09.146>

BIOGRAPHIES

Dr. Aramis Pérez is a Research Fellow at the Energy Center of the Mathematical and Physical Sciences Faculty at the University of Chile, and Professor at the School of Electrical Engineering at the University of Costa Rica. He received his B.Sc. degree and Licentiate degree in Electrical Engineering from the University of Costa Rica. He received his M.Sc. degree in Business Administration with a General Management Major from the same university. He also received the Doctorate in Electrical Engineering degree from the University of Chile. His research interests include parametric/non-parametric modeling, system identification, data analysis, machine learning and manufacturing processes.

Matías Benavides is a graduate student in Electrical Engineering at the Department of Electrical Engineering at the University of Chile, working under the supervision of Dr. Marcos Orchard.

Heraldo Rozas is a graduate student at the Department of Electrical Engineering at the University of Chile, working under the supervision of Dr. Marcos Orchard. His research interests include system identification, estimation theory and decision making under uncertainty.

Sebastián Seria is a graduate student in Electrical Engineering at the Department of Electrical Engineering at the University of Chile, working under the supervision of Dr. Marcos Orchard.

Dr. Marcos E. Orchard is Associate Professor with the Department of Electrical Engineering at Universidad de Chile and was part of the Intelligent Control Systems

Laboratory at The Georgia Institute of Technology. His current research interest is the design, implementation and testing of real-time frameworks for fault diagnosis and failure prognosis, with applications to battery management systems, mining industry, and finance. His fields of expertise include statistical process monitoring, parametric/non-parametric modeling, and system identification. His research work at the Georgia Institute of Technology was the foundation of novel real-time fault diagnosis and failure prognosis approaches based on particle filtering algorithms. He received his Ph.D. and M.S. degrees from The Georgia Institute of Technology, Atlanta, GA, in 2005 and 2007, respectively. He received his B.S. degree (1999) and a Civil Industrial Engineering degree with Electrical Major (2001) from Catholic University of Chile. Dr. Orchard has published more than 100 papers in his areas of expertise.